Blood flow dynamics in the total cavopulmonary connection long-term after Fontan completion

Rijnberg, F.M.

CHAPTER 6B

Four-dimensional flow magnetic resonance imaging-derived blood flow energetics of the inferior vena cava-to-extracardiac conduit junction in Fontan patients

Rijnberg FM, Elbaz MSM, Blom NA, Westenberg JW, Kroft LJ, Kamphuis V, Helbing WA, Hazekamp MG, Roest AAW

European Journal of CardioThoracic Surgery 2019

Abstract

Objectives

In patients with a Fontan circulation, systemic venous return flows passively towards the lungs. Due to an absent subpulmonary ventricle, favorable blood flow patterns with minimal energy loss are clinically relevant. The region where the inferior vena cava, hepatic veins and extracardiac conduit join (IVC-conduit junction) is a potential source of increased energy loss. The aim of this study was to evaluate the relationship between geometry and blood flow patterns in the IVC-conduit junction with associated kinetic energy and energy loss using four-dimensional flow MRI.

Methods

Fourteen extracardiac conduit-Fontan patients underwent four-dimensional flow MRI. IVC-conduit junctions were ranked into 3 groups for 3 categories: geometry, flow complexity and conduit mean velocity. The relative increase in mean velocity from the IVC to conduit (representing IVC-conduit mismatch) was determined. Peak and mean kinetic energy and energy loss were determined and normalized for volume.

Results

In 4/14 patients, adverse geometries led to helical flow patterns and/or acute changes in flow direction. For each category, the most adverse IVC-conduit junctions were associated with an approximate 2.3-3.2 and 2.0-2.9 fold increase in kinetic energy and energy loss, respectively. IVC-conduit mismatch strongly correlated with mean kinetic energy and energy loss ($r=0.80$, $p=0.001$ and $r=0.83$, $p<0.001$, respectively) and with body surface area in patients with 16mm conduits ($r=0.88$, $p=0.010$).

Conclusions

The IVC-conduit junction is a potential source of increased energy loss. Junctions with increased energy loss showed 1) distorted geometry leading to adverse blood flow patterns and/or 2) IVC-conduit mismatch. 16mm conduits appear to be inadequate for older patients.

Introduction

The Fontan procedure is the current palliative approach for children with a univentricular heart defect. After completion of the Fontan circulation (total cavopulmonary connection, TCPC), the systemic venous return flows passively towards the lungs. Due to the absence of a subpulmonary ventricle, favorable blood flow patterns within the Fontan circulation with minimal energy loss are clinically relevant.(1) Previous computational fluid dynamic studies have identified relationships between increased energy loss in the TCPC and decreased exercise capacity(2, 3), altered cardiac function parameters (e.g. cardiac output, diastolic function) (4, 5) and an increased central venous pressure.(6) These studies, however, only modeled blood flow in the TCPC from the level of the Fontan tunnel to the pulmonary arteries. Until now, no studies have reported on energy loss levels in the blood flow in the region below the conduit, where the inferior vena cava (IVC), hepatic veins and conduit join (IVC-conduit junction). Subsequently, little is currently known about the geometry, blood flow patterns and associated energy loss in this region. We hypothesize that within the Fontan circulation, the IVC-conduit junction is another potential source of increased energy loss due to variable geometries.

More knowledge about this region could possibly have implications for diagnostic work-up in Fontan patients, as currently there is little focus on the IVC-conduit junction as a potential region of adverse hemodynamics.

Four-dimensional (4D) flow MRI has emerged as a novel technique capable of assessing in vivo 3D, time-resolved (i.e. over a cardiac cycle) blood flow.(7) 4D flow MRI enables in vivo acquisition of the 3D velocity field needed to visualize the dynamic 3D blood flow patterns and to quantify novel energetic markers.(8) Therefore, the aim of this study was to evaluate the relationship between altered geometry and blood flow patterns in the IVC-conduit junction with associated kinetic energy and energy loss using 4D flow MRI.

Material and methods

Study population

Fourteen extracardiac conduit-Fontan patients were retrospectively selected from a local database comprising both clinical 4D flow MRI examinations (as part of routine follow-up) and 4D flow scans that are part of an ongoing prospective multi-center study. All patients were randomly selected and did not have a clinical indication for the MRI. Patients with sufficient quality 4D flow data (free of motion/clips artifacts) in the IVC-conduit junction region were included. The study was approved by the Medical

Ethical Committee of the Erasmus Medical Center with the local approval of the Leiden University Medical Center. Informed consent was obtained from all participants and/or their legal representatives.

MRI acquisition

4D flow MRI (Ingenia, Philips Healthcare, Best, the Netherlands) of the Fontan circulation was performed at Leiden University Medical Center between May 2014-March 2017. The 4D flow MRI acquisition covered the entire Fontan circulation from the IVC and superior vena cava towards both pulmonary arteries. Acquisition details are summarized in Supplementary Table 1.

4D flow MRI analysis

The area of interest for this study was the IVC-conduit junction, which consists of three parts: 1) the IVC below entry of the hepatic veins (IVC), 2) the area of the IVC where the hepatic veins enter (IVC-HV) and 3) the conduit (Figure 1, Video 1). The hepatic veins were excluded from the analysis due to inadequate spatial resolution of the 4D flow MRI data in these small vessels. The segmentation of the IVC-conduit junction was standardized to allow for comparison of blood flow energetics between cases and comprised 6cm in total, starting at the first 2 cm of the conduit downwards (Figure 1B). The vessel lumen was manually segmented on the phase with the highest contrast on magnitude-weighted speed images of the 4D flow data using in-house developed MASS software, and subsequently propagated towards the other phases.

Ranking of the IVC-conduit junction

To evaluate the impact of differences in geometry, flow patterns and conduit velocities on energetics, the IVC-conduit junction was ranked using 3 categories: geometry, flow complexity and mean velocity in the conduit. For each category, the study group was subdivided into 3 groups as defined below. Segmentations, pathline movies and streamline images were obtained and could be freely rotated in 3D to allow for optimal qualitative assessment of maximum angles and flow patterns used for the ranking (CAAS MR solutions v5.0, Pie Medical Imaging, Maastricht, the Netherlands). The maximum angle between 1) the IVC and the IVC-HV connection (the part of the IVC where the hepatic veins enter the IVC) and 2) between the IVC-HV connection and the conduit, were qualitatively determined (Figure 1B).

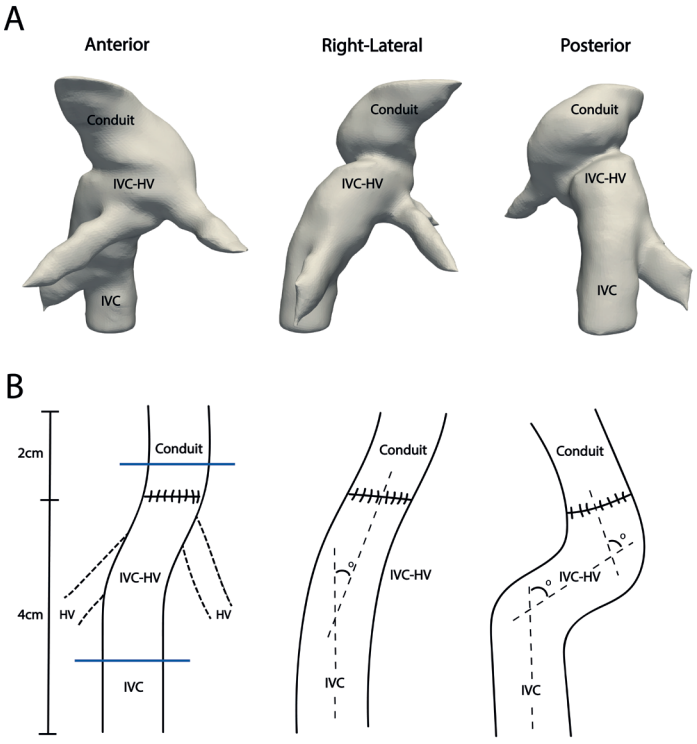

Figure 1. (A) Anterior, right-lateral and posterior view of a distorted IVC-conduit junction in a 12-year old female patient with an 18mm conduit. HVs are included for orientation. **(B)** Schematic representation of the IVC-conduit junction. HVs are shown for orientation **(left image)**. Position of 2D flow planes is shown **(blue lines)**. Angles between the IVC and IVC-HV and IVC-HV and conduit are shown for a relatively straight **(middle image)** and distorted IVC-conduit junction **(right image)**. IVC; inferior vena cava, HV; hepatic veins.

Accordingly, the geometry was divided into three groups based on the sum of above-mentioned angles: 1) a cumulative angle <50°, 2) 50°-90° or 3) >90°. Flow complexity was divided into three groups: 1) well developed flow without helical flow patterns (defined by the curvature of the path- and streamlines representing a corkscrew flow pattern), 2) minor helical flow ≤180° in the majority of pathlines/streamlines or flow distortion (defined as helicity ≥180° or acute (single angle >90°) change in flow direction) in only a small part of the pathlines/streamlines, and 3) helicity≥180° and/or acute change in flow direction of the majority of pathlines/streamlines in the IVC-conduit junction.

To determine the reproducibility of the geometry and flow complexity rankings, the inter- and intraobserver analysis was performed on blinded datasets for all cases. The intraobserver analysis was performed >8 weeks after the first ranking.

IVC-conduit mismatch was defined by an increase in mean velocity from the IVC towards the conduit. Mean velocity in the conduit was arbitrarily grouped into 1) <25cm/s, 2) 25-35cm/s and 3) >35cm/s, with the rationale that higher velocity suggests higher IVC-conduit mismatch when mean velocities in the IVC are similar between groups. In addition, the percentage of IVC-conduit mismatch was also quantified, by assessing the relative increase of mean velocity in the conduit versus IVC for each phase with forward flow ($V_{conduit}$-V_{IVC}/V_{IVC} x 100%, where V is the mean velocity), using 2D planes positioned perpendicular on the 4D flow data of the IVC and conduit (Figure 1B).

Blood flow energetics: viscous energy loss and kinetic energy

The amount of kinetic energy and viscous energy loss in the IVC-conduit junction was computed from 4D flow MRI velocity data using custom developed software.(8) Kinetic energy is the amount of energy the blood flow possesses due to its motion. In short, for each voxel in the IVC-conduit junction, the kinetic energy was computed as $\frac{1}{2}mv^2$, where (m) is the mass of a voxel and (v) is the velocity acquired with 4D flow MRI. The total amount of kinetic energy (in milliJoule, [mJ]) is computed for each phase in the cardiac cycle (i.e. one cardiac cycle is reconstructed into 25-30 phases) by summing the kinetic energy of all voxels within the IVC-conduit junction. The peak kinetic energy (KE_{peak}) represents the phase in the cardiac cycle in which the blood flow contains the most kinetic energy volume and the mean kinetic energy (KE_{mean}) is the kinetic energy volume present in the blood flow averaged over all the phases of the cardiac cycle.

Viscous energy loss is the kinetic energy that is lost due to viscosity-induced frictional forces in the flow and can be computed using the viscous dissipation function, assuming blood flow to be laminar.(1, 8) Of note, helical flow patterns in the Fontan circulation still represent laminar flow from a fluid dynamic perspective (based on Reynolds numbers <2300), as blood flow in the TCPC has been reported to be well within this laminar flow regime.(1, 9, 10)

Similar to kinetic energy, for each phase in the cardiac cycle, the total viscous energy loss rate (in milliWatt, mW) of the blood flow in the IVC-conduit junction was computed. The peak energy loss rate ($\dot{EL}_{peak}$) represents the phase in the cardiac cycle in which the most energy loss volume is present in the blood flow. The mean energy loss rate ($\dot{EL}_{mean}$) represents the energy loss rate volume in the blood flow averaged over all the phases of the cardiac cycle. As total kinetic energy and energy loss amount is proportional to the volume, these parameters were normalized by the segmented IVC-conduit junction volume (norm_KE (J/m^3) and norm_$\dot{EL}$ (W/m^3)), in line with previous studies.(8, 11, 12)

Statistical analysis

Continuous data are presented as median + interquartile range (IQR). Comparisons between energetics between groups were performed using the Kruskal Wallis test with post-hoc Dunn's test for multiple comparisons. Correlation between IVC-conduit mean velocity increase and energetics was assessed using the Pearson correlation coefficient (r) (normal distributed data), or the Spearman correlation coefficient (r) (non-normal distributed data). Inter- and intraobserver variability was tested using the linear weighted Cohen's Kappa test. A P value <0.05 (two-tailed) was considered statistically significant. Data were analyzed with SPSS 24.0 (IBM-SPSS, Chicago, IL) and Prism 7.0 (GraphPad Software, La Jolla, CA).

Results

Baseline characteristics of the study population are presented in Table 1. The IVC-conduit junction was characterized by remarkable differences in geometry, associated flow patterns and/or conduit mean velocity.

Geometry and Flow complexity

Small cumulative angles (<50°, group 1) were present in 6 patients, which was mostly directed in the posterior-anterior direction as the IVC is directed from parallel to the vertebral column towards the more anteriorly situated conduit (Figure 2A). These patients (group 1) showed well developed flow without any associated helical flow patterns or acute changes in flow direction. On the other end of the spectrum (group 3), 4 patients showed a highly distorted geometry, characterized by (cumulative) angles >90° resulting in a distorted and/or spiraling IVC-conduit junction (Figure 1A). These adverse junctions resulted in flow distortion with acute (single angle >90°) changes in flow directions and/or the occurrence of a helical flow pattern (Figure 2C-D). Note how a distorted junction caused a severe helical flow pattern extending into the conduit (Figure 2D). Of note, ranking of the geometry of the IVC-conduit junction showed strong similarities with flow complexity, as these two factors are obviously highly correlated.

The results of kinetic energy and energy loss analysis are presented in Table 2. Kinetic energy and energy loss showed a strong positive correlation (ρ=0.92, p<0.001, figure 3A). Significant differences were present between group 3 and group 1 when categorized by geometry, with a 2.3-2.9 and 2.6-2.9 fold increase in peak and mean kinetic energy and energy loss, respectively, in group 3. When categorized by flow complexity, only peak and mean energy loss was significantly different with a 2.0-2.7 fold increase in group 3 versus group 1. Post-hoc analysis did not show significant differences between group 1-2 and group 2-3 for both categories.

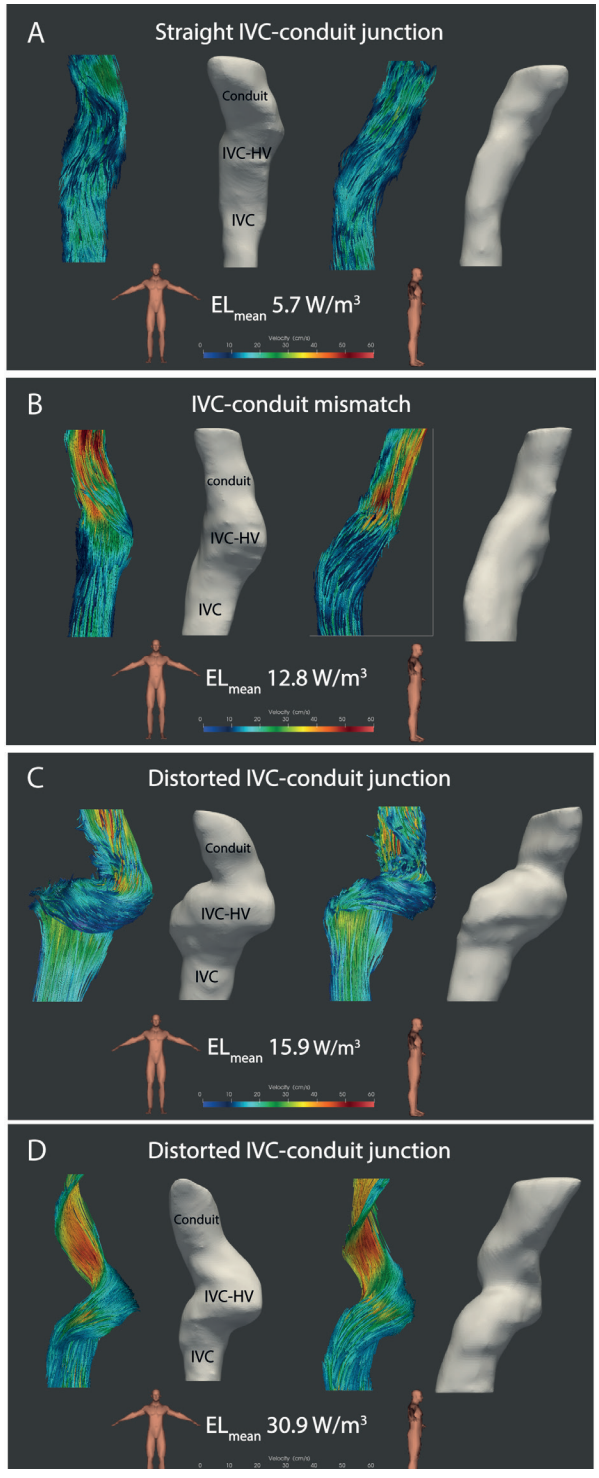
A
Straight IVC-conduit junction
Conduit
IVC-HV
IVC
EL mean 5.7 W/m3
B
IVC-conduit mismatch
conduit
IVC-HV
IVC
EL mean 12.8 W/m3
C
Distorted IVC-conduit junction
Conduit
IVC-HV
IVC
EL mean 15.9 W/m3
D
Distorted IVC-conduit junction
Conduit
IVC-HV
IVC
EL mean 30.9 W/m3

Figure 2. (opposite) Pathline images of 4D flow MRI derived blood flow in the IVC-conduit junction, excluding the HVs, is shown for 4 representative cases. Normalized mean energy loss values (W/m^3) are reported.

(A) IVC-conduit junction of an 11-year old male patient with 18mm conduit. A relatively straight junction is shown with a small angle in the posterior-anterior direction. (B) IVC-conduit junction of an 18-year old female patient with 16mm conduit. A sudden increase in velocity in the conduit is observed, indicating IVC-conduit mismatch. **(C-D)** A distorted IVC-conduit junction is shown in a **(C)** 18-year old female patient with 16mm conduit and a **(D)** 12-year old patient with 18mm conduit. Note how large angles are present in multiple directions creating helical flow patterns with acute changes in flow direction.

Of note, a larger part of the conduit is shown in some figures for visualization purpose only. In the energetic analysis, only a standardized part of the conduit was included (Figure 1B). IVC; inferior vena cava, HV; hepatic veins. W; Watt.

Table 1. Baseline characteristics of the study population

Male, n (%)	5 (36)
Primary diagnosis, n (%):	
HLHS	5 (36)
DILV	2 (14)
DORV +/- TGA +/- cAVSD	3 (21)
TA	2 (14)
Other	1 (7)
Pre-Fontan characteristics	
Age at ECC-Fontan (years)	3.4 (1.3)
Height (cm)	97 (8)
Weight (kg)	14.6 (2.7)
BSA (m^2)	0.64 (0.08)
Pre-MRI characteristics	
Age at 4D flow MRI (years)	14.2 (7.6)
Height (cm)	154 (21)
Weight (kg)	42.0 (19.2)
BSA (m^2)	1.3 (0.4)
Conduit size (16mm/18mm/20mm)	7/5/2
Mean velocity IVC (cm/s)	15.2 (4.0)
Mean velocity ECC (cm/s)	24.5 (16.1)

Values are presented as median (IQR). MRI; magnetic resonance imaging, BSA; body surface area (Haycock), HLHS; hypoplastic left heart syndrome, DILV; double inlet left ventricle, DORV; double outlet right ventricle, TGA; transposition of great arteries, cAVSD; complete atrioventricular septum defect, TA; tricuspid atresia, IVC; inferior vena cava, 4D; four-dimensional

A strong reproducibility of the ranking of the IVC-conduit junction was shown and was equal for both inter- and intraobserver variability (κ=0.921, p<0.001 and κ=0.915, p<0.001 for geometry and flow complexity, respectively). Only 2 patients were ranked differently (1 patient per observer with differences between group 1 and 2 only) compared with the initial ranking.

Mean velocity conduit

Mean velocity in the IVC and conduit are presented in Table 1. Mean velocity in the IVC between the 3 groups of conduit mean velocity was not significantly different (median 13.9 cm/s (6.2), median 15.1 cm/s (1.6) and median 16.2 cm/s (6.7) for groups 1-3, respectively, p=0.243). A 2.7-3.2 and a 2.6 fold increase in peak and mean kinetic energy and energy loss, respectively, was found in group 3 compared with group 1 (Table 2). Post-hoc analysis did not show significant differences between group 1-2 and group 2-3.

Table 2. Impact of geometry, flow complexity and mean conduit velocity on energetics in the IVC-conduit junction

Geometry	**Group 1 (n=6)**	**Group 2 (n=4)**	**Group 3 (n=4)**	**P value**
norm_KE_{mean}(J/m^3)	10.0(4.8)	16.3(9.6)	29.2(10.9)	0.009
norm_KE_{peak}(J/m^3)	14.2(12.3)	24.6(13.6)	33.3(13.4)	0.014
norm_EL_{mean}(W/m^3)	6.0(2.6)	8.5(3.8)	17.2(13.0)	0.007
norm_EL_{peak}(W/m^3)	8.0(6.5)	14.7(7.2)	20.7(17.8)	0.014
Flow Complexity	**Group 1 (n=6)**	**Group 2 (n=5)**	**Group 3 (n=3)a**	**P value**
norm_KE_{mean}(J/m^3)	10.8(12.0)	15.8(12.9)	28.8(21.5-35.9)	0.096
norm_KE_{peak}(J/m^3)	18.6(13.2)	20.3(18.8)	32.8(24.5-42.1)	0.135
norm_EL_{mean}(W/m^3)	6.9(4.7)	8.1(5.2)	18.5(16.0-30.9)	0.034
norm_EL_{peak}(W/m^3)	11.0(7.7)	11.9(9.1)	22.0(19.3-40.4)	0.031
Conduit mean velocity	**Group 1 (n=5)**	**Group 2 (n=4)**	**Group 3 (n=5)**	**P value**
norm_KE_{mean}(J/m^3)	9.1(5.8)	18.1(8.6)	28.8(12.2)	0.016
norm_KE_{peak}(J/m^3)	13.2(6.6)	24.1(5.5)	32.8(11.7)	0.007
norm_EL_{mean}(W/m^3)	5.7(1.9)	8.7(8.6)	14.5(12.6)	0.015
norm_EL_{peak}(W/m^3)	7.0(3.2)	13.2(7.6)	18.6(12.3)	0.007

Values are reported as median (interquartile range). [a]total range. P values represent overall Kruskal Wallis test. *KE; kinetic energy, EL; viscous energy loss, mW; milliWatt, W; Watt, mJ; milliJoule, J; joule, IVC; inferior vena cava*

The mean IVC-conduit mismatch in the study cohort was 55.8% (SD: 48%, range -20% to 167%). One outlier was excluded from the analysis as this case showed helical flow extending into the conduit (Figure 2D). Therefore, 2D through-plane velocity analysis in the conduit significantly underestimated true antegrade velocity in this case, thereby compromising the assessment of the IVC-conduit velocity increase. Results of correlation analysis between IVC-conduit velocity increase and kinetic energy and energy loss are mentioned in Supplementary Table 2, including results with the outlier included for completeness. A strong positive correlation was found between IVC-conduit velocity increase and norm_KE_{mean} (r=0.80, p=0.001, Figure 3B) and norm_$\dot{E}L_{mean}$ (r=0.83, p<0.001, Figure 3C). To determine the effect of body size on IVC-conduit mismatch, correlation analysis was performed between BSA and IVC-conduit velocity increase according to conduit size. A strong correlation was found between BSA and

IVC-conduit velocity increase in the 16mm group (r=0.88, p=0.010, Figure 3D). The groups with 18mm and 20mm conduit size were too small for further evaluation.

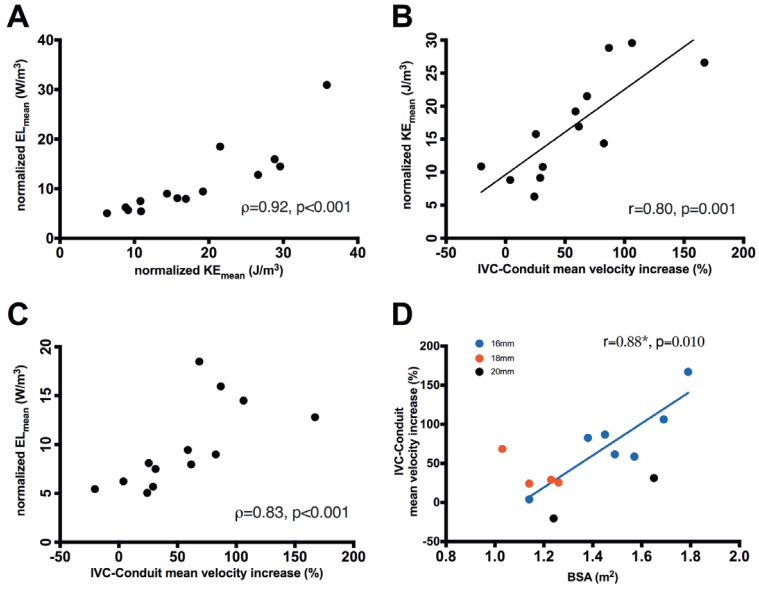

Figure 3. A strong positive correlation is shown between IVC-conduit mean velocity increase (representing IVC-conduit mismatch) and normalized KE_{mean} **(A)** and EL_{mean} **(B)**. A strong positive correlation between normalized KE_{mean} and EL_{mean} is shown **(C)**. A strong positive correlation is shown between IVC-conduit mean velocity increase and BSA in patients with 16mm conduits* **(D)**.

IVC; inferior vena cava, KE; kinetic energy, EL; viscous energy loss, BSA; body surface area, W; Watt, J; Joule

Discussion

The aim of this study was to evaluate the relationship between altered geometry and blood flow patterns in the IVC-conduit junction with associated energetics (kinetic energy and energy loss) using in vivo 4D flow MRI. The main findings show that the IVC-conduit junction is characterized by heterogeneous geometry leading to variable flow patterns. Important characteristics of the junctions associated with adverse energetics were 1) a distorted geometry, characterized by (cumulative) angles >90° resulting in adverse flow patterns with acute changes in flow direction and/or helical flow patterns, and 2) IVC-conduit mismatch. The most adverse junctions showed 2.3-3.2 and 2.0-2.9 fold increase in peak and mean kinetic energy and energy loss, respectively, and these adverse connections are therefore of potential clinical significance in Fontan patients. Furthermore, IVC-conduit mismatch was strongly associated with BSA in patients with

16mm conduits, indicating that these conduits may be inadequate for older Fontan patients.

The geometrical distortion of the IVC-conduit junction we observed in a subset of patients was surprising and it is unclear whether this is caused by natural variability in anatomy of the IVC and IVC-HV region in healthy humans, or is related to the Fontan procedure. Subsequently, longitudinal information of changes in geometry of this region with growth after completion of the Fontan circulation is essential as major changes occur in body composition from Fontan completion to adulthood. Finally, if reintervention is considered after Fontan completion, detailed evaluation of this region is important as this also may be an adverse factor in the complications occurring in these patients which can potentially be optimized.

Our data showed a strong positive correlation between IVC-conduit mismatch and normalized mean kinetic energy and energy loss. Furthermore, a strong positive correlation was present between BSA and IVC-conduit mismatch in patients with 16mm conduits. While the use of 16mm conduits has been reported to provide good short to mid-term results in small-sized patients(13, 14), results in full grown adults remain mostly unknown and, according to our data, may only be sufficient for small adults. In our center, 16mm conduits have been used in the early periods but have been abandoned since many years due to concerns of inadequate size in the long term. Our data seem to justify this approach from an energetic point of view. Basically, optimal conduit size varies with age and is a trade-off situation: in young patients with large conduits, flow expansions at the IVC-conduit junction leads to flow separation which is also associated with increased energy loss. Furthermore, these oversized conduits increase areas of flow stagnation or flow reversal, which potentially increases risk of thrombosis and therefore limits the amount of conduit oversizing by the surgeon.(15) In older, larger patients, energy loss increases if the used conduit becomes too small.(16) As Fontan tunnel diameter has been described as the most important geometric factor of the TCPC associated with increased energy loss, large patients with 16mm conduits may therefore be at increased risk of complications.(1, 17) Importantly, whether 18mm and 20mm conduits will be large enough for the adult Fontan patient could not be investigated in this study due to small sample sizes. The 18mm patients in this study were relatively young with a low BSA and observed IVC-conduit mismatch would increase when these patients grow.

Comparing absolute values of energy loss derived from 4D flow MRI with previous reported in vitro or computational fluid dynamic studies is challenging. On the one hand, 4D flow MRI has been shown to systematically underestimate “true” energy loss compared with computational fluid dynamics due to the limited spatial resolution

of 4D flow MRI.(10) On the other hand, simulated blood flow and energetics using computational fluid dynamic modelling can be influenced by simplified assumptions and boundary conditions.(1) In a study by Cibis et al.(10), the only study to date that calculated viscous energy loss in the Fontan circulation using 4D flow MRI, mean peak energy loss rate was 0.56mW (SD: 0.28) in the TCPC (covering the area from the Fontan tunnel, superior vena cava and both pulmonary arteries). In our study, absolute peak energy loss rate in the IVC-conduit junction was a median of 0.26 mW with a total range of 0.11-0.94mW, and may therefore be a relevant, previously unidentified source of energy loss in the Fontan circulation.

In the past decades, extensive knowledge has been acquired with in vitro and computer models about the effect of TCPC geometry on energy loss.(1, 3, 4, 6, 9) Energy loss in the TCPC has been linked to several clinically important complications seen in Fontan patients, including a reduced exercise capacity and altered cardiac function parameters.(1, 2, 4, 6) Increased energy loss (resistance) results in elevated central venous pressure(6), which is an important factor in the pathogenesis of the well-known upstream Fontan complications, including liver fibrosis/cirrhosis, protein losing enteropathy or veno-venous collateral formation.(18, 19) To date, various energy-consuming geometric factors of the TCPC have been identified (e.g. small pulmonary artery size(20)) and our data suggest that the IVC-conduit junction is an additional geometric factor with potential increased energy loss. Future studies with larger sample sizes are necessary to better clarify the role of adverse geometry and blood flow patterns in the IVC-conduit junction and TCPC on adverse outcome in Fontan patients. Evaluation of the Fontan circulation using 4D flow MRI is promising, by directly measuring *in vivo* energy loss from 4D blood flow data, and may be of particular interest in failing Fontan patients(21), as these patients in particular may have adverse geometries and/or blood flow patterns which can be optimized by surgical or catheter-based intervention.

Limitations

This study is limited by a small sample size, but represents randomly selected Fontan patients. Furthermore, different mechanisms of energy loss (IVC-conduit mismatch and distorted geometry with abnormal flow patterns) could occur simultaneously, making the relative contribution of each mechanism on calculated energetics difficult. Two patients underwent 4D flow MRI on a 1.5T scanner and lower signal-to-noise ratio in these patients may have affected calculated energetics. Analysis was performed on a static segmentation of the IVC-conduit junction and minor movement between phases may have introduced small errors. However, this may have been present in the same order of magnitude in all patients. The 4D flow MRI protocol used free-breathing with no respiratory gating, and therefore no distinction between inspiration and expiration

flow data can be made. As such, the influence of respiration on observed flow patterns and energetics could not be assessed in this study.

Conclusions

In conclusion, the IVC-conduit junction is a currently undervalued source of increased energy loss. The most adverse junctions show a probable clinically relevant 2.3-3.8 and 2.0-3.5 fold increase in kinetic energy and energy loss, respectively. Identified mechanisms of energy loss are 1) distorted geometry leading to adverse blood flow patterns, and 2) IVC-conduit mismatch. IVC-conduit mismatch was strongly correlated with kinetic energy and energy loss. Furthermore, IVC-conduit mismatch strongly correlated with BSA in patients with 16mm conduits, indicating that these conduits may be inadequate for adult Fontan patients. Therefore, these patients are potentially at increased risk for experiencing complications. Whether 18mm and 20mm conduits will be large enough could not be determined due to small sample size and is subject to future studies. Larger sample sizes are warranted to further clarify the importance of adverse IVC-conduit junctions on long-term clinical outcome.

References

1. Rijnberg FM, Hazekamp MG, Wentzel JJ, de Koning PJH, Westenberg JJM, Jongbloed MRM, et al. Energetics of Blood Flow in Cardiovascular Disease: Concept and Clinical Implications of Adverse Energetics in Patients With a Fontan Circulation. Circulation. 2018;137(22):2393-407.
2. Khiabani RH, Whitehead KK, Han D, Restrepo M, Tang E, Bethel J, et al. Exercise capacity in single-ventricle patients after Fontan correlates with haemodynamic energy loss in TCPC. Heart. 2015;101(2):139-43.
3. Tang E, Wei ZA, Whitehead KK, Khiabani RH, Restrepo M, Mirabella L, et al. Effect of Fontan geometry on exercise haemodynamics and its potential implications. Heart. 2017;103(22):1806-12.
4. Haggerty CM, Whitehead KK, Bethel J, Fogel MA, Yoganathan AP. Relationship of single ventricle filling and preload to total cavopulmonary connection hemodynamics. Ann Thorac Surg. 2015;99(3):911-7.
5. Honda T, Itatani K, Takanashi M, Mineo E, Kitagawa A, Ando H, et al. Quantitative evaluation of hemodynamics in the Fontan circulation: a cross-sectional study measuring energy loss in vivo. Pediatr Cardiol. 2014;35(2):361-7.
6. Sundareswaran KS, Pekkan K, Dasi LP, Whitehead K, Sharma S, Kanter KR, et al. The total cavopulmonary connection resistance: a significant impact on single ventricle hemodynamics at rest and exercise. Am J Physiol Heart Circ Physiol. 2008;295(6):H2427-35.
7. Kamphuis VP, Westenberg JJM, van der Palen RLF, Blom NA, de Roos A, van der Geest R, et al. Unravelling cardiovascular disease using four dimensional flow cardiovascular magnetic resonance. Int J Cardiovasc Imaging. 2017;33(7):1069-81.
8. Elbaz MS, van der Geest RJ, Calkoen EE, de Roos A, Lelieveldt BP, Roest AA, et al. Assessment of viscous energy loss and the association with three-dimensional vortex ring formation in left ventricular inflow: In vivo evaluation using four-dimensional flow MRI. Magn Reson Med. 2017;77(2):794-805.
9. Bossers SS, Cibis M, Gijsen FJ, Schokking M, Strengers JL, Verhaart RF, et al. Computational fluid dynamics in Fontan patients to evaluate power loss during simulated exercise. Heart. 2014;100(9):696-701.
10. Cibis M, Jarvis K, Markl M, Rose M, Rigsby C, Barker AJ, et al. The effect of resolution on viscous dissipation measured with 4D flow MRI in patients with Fontan circulation: Evaluation using computational fluid dynamics. J Biomech. 2015;48(12):2984-9.
11. Kamphuis VP, Elbaz MSM, van den Boogaard PJ, Kroft LJM, van der Geest RJ, de Roos A, et al. Disproportionate intraventricular viscous energy loss in Fontan patients: analysis by 4D flow MRI. Eur Heart J Cardiovasc Imaging. 2018.
12. Kamphuis VP, Westenberg JJM, van der Palen RLF, van den Boogaard PJ, van der Geest RJ, de Roos A, et al. Scan-rescan reproducibility of diastolic left ventricular kinetic energy, viscous energy loss and vorticity assessment using 4D flow MRI: analysis in healthy subjects. Int J Cardiovasc Imaging. 2018;34(6):905-20.
13. Cho S, Kim WH, Choi ES, Kwak JG, Chang HW, Hyun K, et al. Outcomes after extracardiac Fontan procedure with a 16-mm polytetrafluoroethylene conduit. Eur J Cardio-Thorac. 2018;53(1):269-75.
14. Ikai A, Fujimoto Y, Hirose K, Ota N, Tosaka Y, Nakata T, et al. Feasibility of the extracardiac conduit Fontan procedure in patients weighing less than 10 kilograms. J Thorac Cardiov Sur. 2008;135(5):1145-52.

15. Lardo AC, Webber SA, Friehs I, del Nido PJ, Cape EG. Fluid dynamic comparison of intra-atrial and extracardiac total cavopulmonary connections. J Thorac Cardiovasc Surg. 1999;117(4):697-704.
16. Itatani K, Miyaji K, Tomoyasu T, Nakahata Y, Ohara K, Takamoto S, et al. Optimal conduit size of the extracardiac Fontan operation based on energy loss and flow stagnation. Ann Thorac Surg. 2009;88(2):565-72; discussion 72-3.
17. Tang E, Restrepo M, Haggerty CM, Mirabella L, Bethel J, Whitehead KK, et al. Geometric characterization of patient-specific total cavopulmonary connections and its relationship to hemodynamics. JACC Cardiovasc Imaging. 2014;7(3):215-24.
18. Ohuchi H, Yasuda K, Miyazaki A, Kitano M, Sakaguchi H, Yazaki S, et al. Haemodynamic characteristics before and after the onset of protein losing enteropathy in patients after the Fontan operation. Eur J Cardiothorac Surg. 2013;43(3):e49-57.
19. Rychik J, Veldtman G, Rand E, Russo P, Rome JJ, Krok K, et al. The precarious state of the liver after a Fontan operation: summary of a multidisciplinary symposium. Pediatr Cardiol. 2012;33(7):1001-12.
20. Dasi LP, Krishnankuttyrema R, Kitajima HD, Pekkan K, Sundareswaran KS, Fogel M, et al. Fontan hemodynamics: importance of pulmonary artery diameter. J Thorac Cardiovasc Surg. 2009;137(3):560-4.
21. Deal BJ, Jacobs ML. Management of the failing Fontan circulation. Heart. 2012;98(14):1098-104.

Supplementary materials

Supplementary Table 1. 4D flow MRI acquisition details

Field strength (n)	1.5T (2), 3T (12)
Respiratory compensation	none
Cardiac gating	retrospective, 25-30 phases
Spatial resolution (mm)	2.5x2.5x2.5
Temporal resolution (ms)	31.4 (1.6)
Flip angle (°)	10
TE (ms)	3.9±0.2)
TR (ms)	7.9±0.4)
VENC (cm/s)	80
Scan duration (minutes)	8-10
Acceleration methods	SENSE factor 2, AP direction EPI factor 5

Values are represented as mean (SD).

T; Tesla, ms; miliseconds, TE; echo time, TR; repetition time, VENC; velocity encoding, SENSE; sensitivity encoding, AP; anterior-posterior, EPI; echo planar imaging readout.

Supplementary Table 2. Correlation between IVC-conduit velocity increase and energetics

Blood flow energetics	Correlation coefficient	p value	Correlation coefficient (outlier included)	p value
norm_KE_mean (J/m^3)	0.80[a]	0.001	0.69[a]	0.007
norm_KE_peak (J/m^3)	0.78[a]	0.002	0.52[a]	0.057
norm_EL_mean (W/m^3)	0.83[b]	<0.001	0.70[b]	0.006
norm_EL_peak (W/m^3)	0.73[b]	0.005	0.53[b]	0.054

[a]Pearson correlation coefficient, [b]Spearman's rank coefficient

KE; kinetic energy, EL, viscous energy loss, mW; milliWatt, W; Watt, mJ; milliJoule, J; joule, IVC; inferior vena cava